Tellus
SERIES B
CHEMICAL
AND PHYSICAL
METEOROLOGY
PUBLISHED BY THE INTERNATIONAL METEOROLOGICAL INSTITUTE IN STOCKHOLM

Tellus (2011), 63B, 117–128
Printed in Singapore. All rights reserved

TELLUS

Characterization and sources of aerosol particles over the southeastern Tibetan Plateau during the Southeast Asia biomass-burning season

By GUENTER ENGLING[1,2], YI-NAN ZHANG[3], CHUEN-YU CHAN[3,*], XUE-FANG SANG[3], MANG LIN[3], KIN-FAI HO[4], YOK-SHEUNG LI[4], CHUAN-YAO LIN[1] and JAMES J. LEE[5],
[1]*Research Center for Environmental Changes, Academia Sinica, Taipei, Taiwan;* [2]*Department of Biomedical Engineering and Environmental Sciences, National Tsing Hua University, Hsinchu, Taiwan;* [3]*School of Environmental Science and Engineering, Sun Yat-Sen University, Guangzhou, China;* [4]*Department of Civil and Structural Engineering, The Hong Kong Polytechnic University, Hong Kong, China;* [5]*Department of Safety, Health and Environmental Engineering, National Yunlin University of Science, Douliou, Yunlin County, Taiwan*

(Manuscript received 24 December 2009; in final form 16 September 2010)

ABSTRACT

The Tibetan Plateau is one of the highest regions in the world, exerting profound influence on the large-scale atmospheric circulation of Asia and the global climate. Here we report ambient concentrations of black carbon (BC), aerosol mass ($PM_{2.5}$ and PM_{10}) and associated carbonaceous species and water-soluble inorganic ions from a remote mountain site in the southeastern part of the Tibetan Plateau during spring, in order to characterize the major sources contributing to the ambient aerosol in the background atmosphere of Southeast Asia. Significant build-up of aerosol and BC concentrations was observed during a dry period, accompanied by the occurrence of fires and transport of pollution from the nearby regions of Southeast Asia and the northern part of the Indian Peninsula. The concentrations of BC, $PM_{2.5}$ and PM_{10} mass reached maximum hourly values of 1470 ng m^{-3}, 107 and 117 μg m^{-3}, respectively. Organic carbon (OC), elemental carbon (EC) and sulfate were the predominant aerosol components. OC showed strong correlations with EC ($R^2 = 0.93$ for $PM_{2.5}$ and 0.74 for PM_{10}) and non-sea-salt potassium, especially in fine aerosol ($R^2 = 0.95$). In addition, the relative change rates of K^+ against OC reached characteristically high values, highlighting the important contributions of biomass-burning smoke.

1. Introduction

In recent years, increasing scientific attention has been directed to atmospheric aerosols, which comprise a complex mixture of inorganic (including sulfates, nitrates, sea salt and mineral dust) and carbonaceous (organic carbon, OC and elemental carbon, EC) material. While OC is comprised of thousands of individual organic compounds, EC consists of a fairly simple graphite-like carbon skeleton (Andreae and Gelencsér, 2006). Furthermore, black carbon (BC) is a type of carbonaceous material that is at times incorrectly considered equivalent to EC. Although the fundamental molecular composition is similar, these two refractory carbonaceous species are distinguished based on their properties: BC is considered by its atmospheric effects, as it effectively absorbs light across the entire solar spectrum, whereas EC is defined by its elemental composition (Gelencsér, 2004). BC is typically determined by optical methods, whereas EC is measured with thermal techniques. The most commonly used instrument for BC measurement is the aethalometer, which continuously measures light attenuation through a moving filter tape on which aerosol particles are collected (Hansen et al., 1984). On the other hand, EC is typically quantified off-line on quartz-fiber filters by thermo-optical methods (Chow et al., 1993). Different optical correction procedures have been developed to correct for charring bias of a certain OC fraction. Nevertheless, differences in OC and EC measurements can be rather large between different instrumental approaches. Moreover, EC and BC values are not directly comparable because of their fundamentally different measurement principles, while both EC and BC values are associated with their inherent measurement uncertainties. However, superior measurement techniques have been developed recently,

*Corresponding author.
e-mail: chzy@mail.sysu.edu.cn
DOI: 10.1111/j.1600-0889.2010.00512.x

which can significantly reduce the uncertainties associated with BC determination (Slowik et al., 2007). Accurate measurement of BC is crucial, as recent studies have indicated the significant effect of BC on the radiative budget of the earth. BC is the principal component of atmospheric aerosols that absorbs sunlight and therefore contributes to the warming of the atmosphere, unlike most other aerosol components, which scatter incident sunlight and thus have a global cooling effect (Hansen et al., 2001; Ramanathan and Carmichael, 2008).

BC is commonly produced during incomplete combustion, such as during low-temperature burning of agricultural biomass, household biofuels and coal, as well as from diesel engines. BC emissions are particularly large in developing countries, including India and China (Menon et al., 2002). South and Southeast (SE) Asia are two of the major regions in the world with biomass-burning activities (Chan et al., 2003; Duncan et al., 2003). For example, Rengarajan et al. (2007) and Ram et al. (2008) showed that biomass burning was the dominant source for OC in northern India. Consequently, substantial amounts of pollutants are emitted into the atmosphere in each dry season from the South and SE Asian subcontinent as a result of natural forest fires and human initiated burning activities, such as burning of agricultural residues (Sheesley et al., 2003; Streets et al., 2003; Gadde et al., 2009).

The sources and influence of biomass-burning activities in South and SE Asia on regional air quality and climate have been studied extensively, specifically as part of the Atmospheric Brown Cloud project (Ramanathan et al., 2007; Stone et al., 2007; Gustafsson et al., 2009; Stone et al., 2010). These investigations showed that the main sources of BC (or EC) in South and SE Asia were biomass burning and fossil fuel combustion. The resulting smoke emissions are commonly transported to the Indian Ocean and beyond, forming a vast, regional-scale haze layer (Engling and Gelencsér, 2010). The Indian Ocean Experiment also revealed large-scale air pollution in South and SE Asia, extending to the Indian Ocean Inter-Tropical Convergence Zone (Lelieveld et al., 2001). Furthermore, the Transport and Chemical Evolution over the Pacific aircraft campaign showed that significant amounts of aerosol and trace gases of radiative and chemical importance are being transported to South China and the northwestern Pacific (Chan et al., 2003; Jacob et al., 2003). Li et al. (2005) reported elevated CO concentrations and dense clouds over the Tibetan Plateau and southwest China and suggested that these observations were a result of the accumulation of pollutants originating from northeast India and southwest China. In fact, during several independent studies not only in industrial cities, but also in tropical coastal areas and high-altitude locations of northern India BC concentrations were observed at μg m^{-3} levels (Babu and Moorthy, 2002; Tripathi et al., 2005; Pant et al., 2006). These findings highlight the possible impact of emissions from South and SE Asia on the atmospheric composition and regional climate change of the vulnerable ecosystem of the Tibetan Plateau (Wang et al., 2008), calling for more scientific attention. However, over the inland areas of Asia, such as the Tibetan Plateau, which exerts profound influence on the regional and global radiative budget and climate (Ye and Wu, 1998; Ma et al., 2009), systematic and extensive observations of trace gases, aerosol particles and BC in particular, are very limited (Chan et al., 2006; Qu et al., 2008; Zhang et al., 2008).

In this paper, we present the measurement results from a mountain site on the Tibetan Plateau in southwest China during spring, close to the active fire regions of SE Asia and the Indian subcontinent. The intensive campaign included measurements of $PM_{2.5}$ and PM_{10} mass concentrations, concurrent with BC and aerosol chemical composition, obtained by continuous aerosol analysers and filter-based samplers. The chemical characteristics were investigated in form of OC, EC, BC, water-soluble inorganic ions and their mutual correlations. Furthermore, possible sources of aerosols and BC in particular in this part of the Tibetan Plateau were examined and discussed.

2. Experimental methods

2.1. Field measurements

The measurement site was located on the southeastern edge of the Tibetan Plateau in Tengchong County, Yunnan Province. This part of the plateau has an average altitude of 1640 m above sea level (a.s.l.). The monitoring station was situated on top of a mountain (25.01 °N, 98.30 °E, 1960 m a.s.l.), approximately 15 km away from the centre of Tengchong City, 60 km to the east of the Myanmar border and 750 km to the west of Kunming, the capital of Yunnan Province (Fig. 1). There were no significant local emission sources in the area near the station, other than a few small villages and tea plantations in the surrounding hills. In fact, in this remote part of southwest China, local industrial operations and automobile traffic are very limited. The sampling inlet of the continuous analysers was placed 3 m above ground level on the roof of a meteorological station. The measurements were conducted from 7 April to 24 May, 2004, coinciding with the annual intensive biomass-burning season in South and SE Asia (Streets et al., 2003).

$PM_{2.5}$ and PM_{10} mass concentrations were measured by DustTrak monitors (Model 8520, TSI, Shoreview, MN, USA) with a particle size range from 0.1 to approximately 10 μm. The monitors were calibrated against standard gravimetric samplers (Tapered Element Oscillating Microbalance, TEOM Model 1400a, R&P, Albany, NY, USA), specified in the Federal Reference Method, before being deployed for observation. $PM_{2.5}$ and PM_{10} mass concentrations were measured at a flow rate of 1.7 L min^{-1} as 5-min average values. The aerosol mass concentrations obtained by the continuous monitors, however, were converted to filter-based concentrations according to the linear regression relations between the simultaneously measured values by the continuous PM analysers and Mini-Vol samplers, using the following equations: $y = 0.71x + 10.0$ ($R^2 = 0.75$)

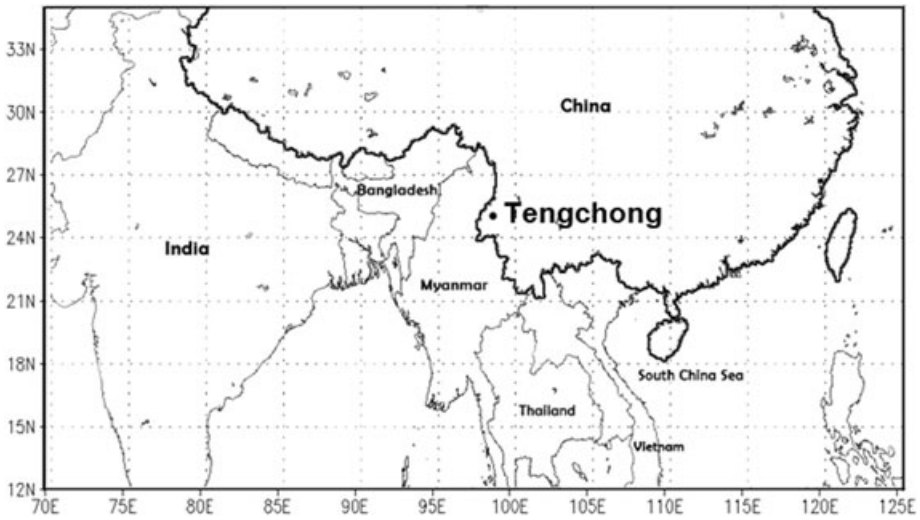

Fig. 1. Map showing the location of the sampling site in Yunnan Province, China and neighbouring countries.

and $y = 0.68x + 9.2$ ($R^2 = 0.65$) for $PM_{2.5}$ and PM_{10}, respectively. BC concentrations were determined by an Aethalometer (Model AE-21, Magee Scientific, Berkeley, CA, USA) with a total suspended particulate inlet and a sampling flow rate of 3.3 L min^{-1}. Similar to the $PM_{2.5}$ and PM_{10} mass concentrations measured by the DustTrak monitors, BC data were recorded as 5-min averages, from which hourly data were derived.

Filter-based $PM_{2.5}$ and PM_{10} samples were collected by a pair of Mini-Vol air samplers (Airmetrics, Eugene, OR, USA) on 47 mm quartz microfibre filters (Whatman QM/A, Piscataway, NJ, USA). The filters were preheated at 800°C for 3 h before use and were placed in clean polyethylene petri dishes, sealed with Teflon tape, before and after field measurements. The Mini-Vol samplers were operated at a flow rate of 5 ± 0.5 L min^{-1}. The sampling duration was 24 h at the beginning and was extended to 48 h in the later part of the campaign, when aerosol concentrations were lower.

2.2. Chemical analysis

All sample filters were stored in petri dishes in a refrigerator at 4 °C, after conditioning and weighing, until chemical analysis to prevent loss of volatile components due to evaporation. Twenty of 52 sample filters (10 pairs of PM_{10} and $PM_{2.5}$ samples, due to limited resources) were analysed for carbonaceous material (OC and EC) by an OC/EC analyser (DRI Thermal/Optical Carbon Analyser, Model 2001) using the IMPROVE thermal/optical reflectance protocol, described by Chow and Watson (2002). A 0.526-cm^2 punch of each quartz filter was analysed for OC and EC according to a procedure similar to that described by Cao et al. (2007).

The remaining filter portions were subject to further analysis of water-soluble inorganic ions. A quarter of each sample filter was extracted with 20 ml of ultra-pure water for 15 min under ultrasonic agitation. Major ionic species (e.g. Na^+, NH_4^+, K^+, NO_3^- and SO_4^{2-}) were measured by ion chromatography (Dionex ICS-2500, Sunnyvale, CA, USA). Dionex CS12 and AS14 columns were used for the separation of cations and anions, respectively. A more detailed description of the analytical procedures as well as the quality control measures, which included analysing field blanks and replicate checks every 10 samples, can be found in Lai et al. (2007).

2.3. Satellite data and trajectory analysis

Fire count maps, displaying the active burning hot spots, were derived from MODIS (Moderate Resolution Imaging Spectroradiometer) satellite images. The data were analysed using a standard MODIS MOD14 Fire and Thermal Anomalies Product algorithm (http://modis.gsfc.nasa.gov/data/dataprod/dataproducts.php?MOD_NUMBER=14). In addition, backward air mass trajectories were used to trace the origins and transport pathways of pollutants from the surrounding regions, including the active biomass-burning areas in SE Asia, to the monitoring site. The 10-day backward air trajectories were obtained by the National Oceanic and Atmospheric Administration (NOAA) HYSPLIT Model (http://www.arl.noaa.gov/ready/hysplit4.html). The model used data from the National Centre of Environmental Prediction reanalysis as input, which have a time resolution of 6 h, a horizontal resolution of 1 degree and a vertical resolution of 27 layers.

3. Results and discussion

3.1. Aerosol mass and BC concentration variations

The statistical distributions of the BC and aerosol mass concentrations, measured by continuous analysers, are summarized in Table 1. $PM_{2.5}$, PM_{10} and BC had overall hourly average

Table 1. Measurement statistics of aerosol mass and BC during the entire sampling period

	Concentrations				Sample No.
	Mean	Stdev.	Min.	Max.	Days/hours
PM_{10} (μg m^{-3})	32	27	9	96	37/877
$PM_{2.5}$ (μg m^{-3})	30	24	10	85	37/877
BC (ng m^{-3})	420	244	43	1471	38/907

concentrations of 30 μg m^{-3}, 32 μg m^{-3} and 420 ng m^{-3}, respectively. The PM mass and BC concentrations exhibited large variations during the experimental period, as shown in Fig. 2, displaying the daily average concentrations from the real-time analysers and daily rainfall record. Low aerosol and BC concentrations were observed in mid April and at the end of the experiment period, when the monitoring station and the neighbouring region experienced extensive rainfall, particularly during 15–18 April and 11–14 May (Fig. 2). The $PM_{2.5}$, PM_{10} and BC values in the first period (15–18 April) ranged from only 15.4–20.0 μg m^{-3}, 14.7–24.5 μg m^{-3} and 140–255 ng m^{-3}, respectively. Meanwhile, there was significant build-up of $PM_{2.5}$, PM_{10} and BC concentrations, averaging at 34 μg m^{-3}, 41 μg m^{-3} and 476 ng m^{-3}, in between the low concentration periods, when fine weather prevailed, until maximum daily averages of 65.5 and 73.8 μg m^{-3} for $PM_{2.5}$ and PM_{10} and 1005 ng m^{-3} for BC were reached between 6 and 10 May. This pattern was also apparent in the concentrations of gaseous pollutants, including CO, NO_y and ozone (Chan et al., 2006). The reverse relationship between rainfall and aerosol, BC and trace gas concentrations is obviously due to scavenging effects of the rain, as well as reduced regional biomass-burning emissions during rainy days (Chan et al., 2006), which will be discussed in later sections.

A well-defined diurnal variation in the aerosol mass and BC concentrations was observed throughout the study period with a broad nocturnal maximum from around 21:00 to 02:00 local standard time (LST; Fig. 3). The aerosol mass and BC concentrations decreased gradually to reach a minimum in the early morning around 05:00 LST, followed by a sharp increase to reach daytime peak concentrations from 08:00–09:00 LST. Following this secondary peak, concentrations of aerosol mass and BC decreased again gradually and subsequently a diurnal minimum was attained in the afternoon (15:00–16:00). Such nocturnal peak and mid-afternoon low concentrations of BC were very similar to those observed at a tropical coastal

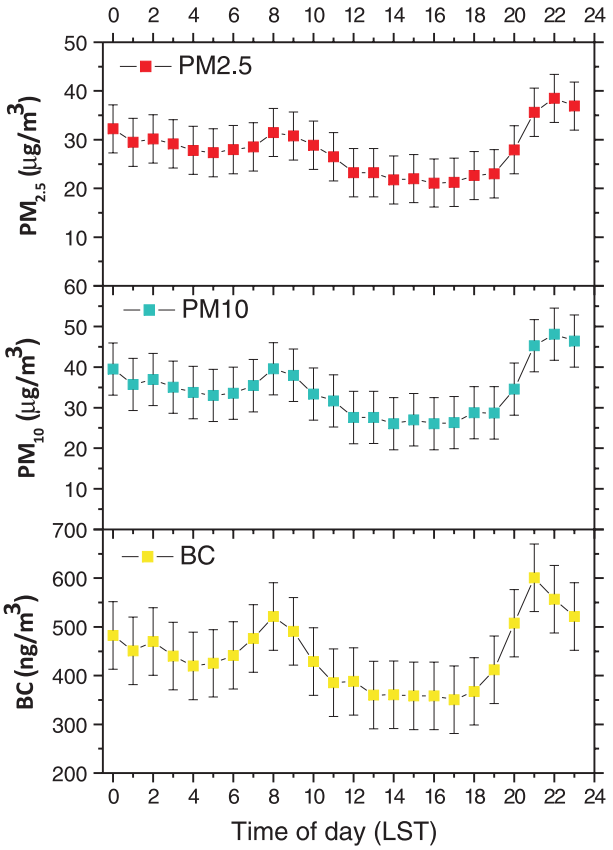

Fig. 3. Average diurnal variations of $PM_{2.5}$ and PM_{10} mass and BC concentrations.

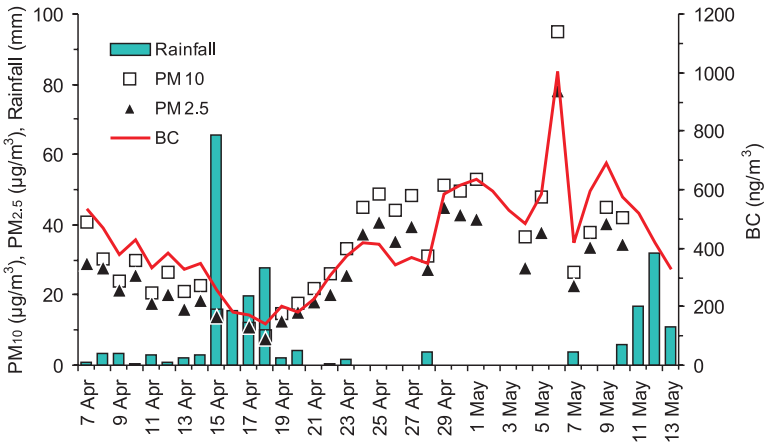

Fig. 2. Daily average concentrations of $PM_{2.5}$ and PM_{10} mass and BC, as well as rainfall throughout the experiment period.

location in India and a continental site in northern India (Babu and Moorthy, 2002; Tripathi et al., 2005), as well as those at an urban site in Xi'an, China (Cao et al., 2009) and those at a suburban site in Maryland, USA (Chen et al., 2001). However, at the remote continental site where this study was conducted, such diurnal variation patterns of aerosol mass and BC concentrations may be explained mainly by the enhanced atmospheric dispersion capacity during daytime and establishment of a shallow and more stable nocturnal boundary layer due to the radiative heating and cooling of the underlying surface by the sun in a diurnal cycle (Cao et al., 2009). In addition, the concentration increases in the morning and the late evening peak were possibly also influenced to some extent by emissions from residential activities, such as cooking and heating, in the surrounding villages, although the population in the vicinity of the sampling site was very scarce and there were no industrial or traffic operations.

3.2. *Episodic events of aerosol and BC enhancements*

The build-up of aerosol mass and BC concentrations was especially pronounced during two periods with elevated pollution: 23–28 April and 5–10 May (Fig. 4). During the first episode, $PM_{2.5}$ and PM_{10} mass as well as BC concentrations increased substantially, reaching peak values at late night hours of those days. The maximum hourly average concentrations of $PM_{2.5}$, PM_{10} and BC were 107.6 μg m^{-3}, 116.2 μg m^{-3} and 1223 ng m^{-3}, respectively, on 24 April and similar values were observed on 26 April. In the second episode, $PM_{2.5}$, PM_{10} and BC concentrations increased drastically, starting in the evening of 5 May and attained peak levels in the early morning of 6 May. High concentrations were sustained until early afternoon of 6 May, forming a broad high pollution regime. The maximum concentrations of $PM_{2.5}$, PM_{10} and BC during this episode were 98.6 μg m^{-3}, 107.1 μg m^{-3} and 1470 ng m^{-3}, respectively. These enhanced values in aerosol mass and BC in particular attained magnitudes close to the levels reported for urban areas of some large Asian cities, such as Guangzhou (Cao et al., 2007). It may be reasonable to state that there was continuous build-up of pollutants throughout most of the observation period until the onset of the rainy season, indicating the extended influence of biomass burning and other possible anthropogenic activities in South and SE Asia on the Tibetan Plateau during spring time.

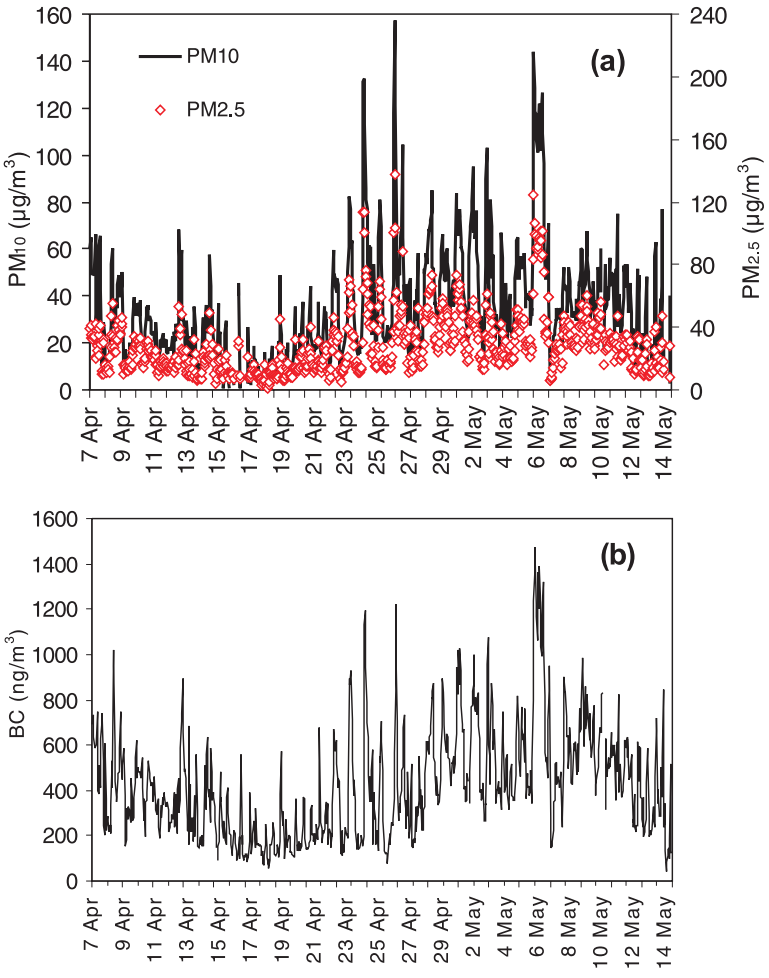

Fig. 4. Hourly concentrations of $PM_{2.5}$ and PM_{10} mass (a) and BC (b) during the entire experiment period.

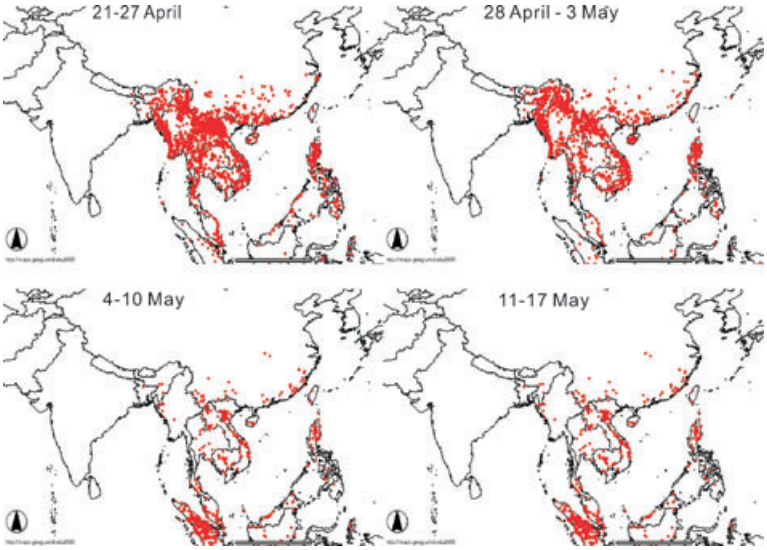

Fig. 5. Geographical distribution of 7-day composite fire hot spots in SE Asia on 21–27 April, 28 April–3 May, 4–10 May and 11–17 May derived from MODIS satellite data.

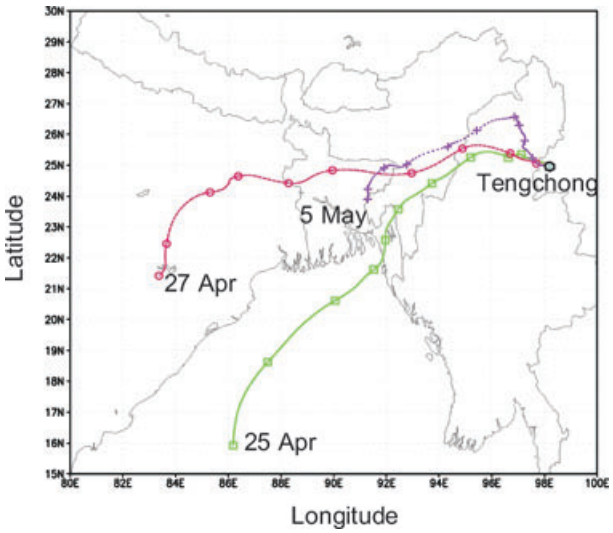

Fig. 6. Backward air mass trajectories reaching the monitoring site at 800 m above local ground level on 25 and 27 April and 5 May.

During the dry period from 21 April to 10 May, which included the episodic events mentioned above, extensive fire activities occurred in the northern part of the SE Asian subcontinent, close to the Chinese border, as illustrated in the 7-day fire count maps (Fig. 5). Compared to the fire counts during 21–27 April and 28 April–3 May, there was significantly reduced burning activity during the later part of the campaign, coinciding with rainy weather. The 10-day backward air mass trajectories for 25 and 27 April and 5 May (Fig. 6), when the highest aerosol mass and BC levels were recorded, showed that the polluted air masses originated from the Bay of Bengal, that is, the eastern part of the Indian Peninsula, on 25 April and 5 May and the northeastern part of India on 27 April. All air masses had passed over the active fire regions, including Bangladesh, Myanmar and northeastern India (Fig. 6). In contrast, the air masses coming from the east during periods with lower aerosol concentrations (not shown) originated over the South China Sea. Backward trajectories at other heights and different times of day showed similar patterns, thus confirming the pathways of the air masses reaching the sampling site.

3.3. *Comparison of BC values with literature reports*

It is meaningful to compare the BC values at Tengchong with those from other rural or remote areas in China, as BC measurements are limited in the southeastern part of the Tibetan Plateau. Detailed comparisons of carbonaceous species for China and other parts of the world are available in the literature (Cao et al., 2003, 2007). The BC concentrations measured at Tengchong (with an average of 420 ng m^{-3} over the entire study period) fall within the range of those reported for background locations worldwide, while they were somewhat higher than those observed at American and European mountain background sites. Ahmed et al. (2009) reported average BC levels of 215 ng m^{-3} at a mountain site (1500 m a.s.l.) in New York state, USA. Marinoni et al. (2008) showed that monthly average BC values varied from 120 to 450 ng m^{-3} at Monte Cimone in the northern Italian Apennines. On the other hand, the BC concentrations at Tengchong were substantially lower than those reported for background sites in eastern China. For example, BC was observed with a range of 200 to 3300 ng m^{-3} at Linan, a regional background station in the Yangtze River Delta (central-eastern China) (Tang et al., 1999) and with an annual average of 2400 ng m^{-3} at a rural site in Hong Kong, SE China (Cheng et al., 2006). Similarly, the BC values observed at Tengchong were lower than those reported for Trivandrum, India (>500 ng m^{-3} in April and May, 2000–2001; Babu and Moorthy, 2002) and Bukit Tinggi (864 m a.s.l.), a mountain site in Sumatra with

a yearly average BC concentration of 660 ng m^{-3} (Maenhaut et al., 2002). Most of these measurement sites were located in relatively close proximity to urban areas, which explains the higher regional background concentrations.

In contrast, the average BC concentrations measured in this part of the Tibetan Plateau were higher than those reported for April and May, 1995 (237.0 and 301.1 ng m^{-3}) at Waliguan Observatory (100.90 °E, 36.28 °N), located in the northeastern part of the Tibetan Plateau (Tang et al., 1999). More recent observations in the southeastern part of the Tibetan Plateau were made at a background site in Zhuzhang, Shangri-La County in Yunnan Province, by Qu et al. (2008), although only EC values were reported from that study (BC concentrations were not given). It is worthwhile to mention, however, that the average EC concentrations in PM_{10} observed at Zhuzhang (0.35 μg m^{-3}) were substantially lower compared to those from Tengchong (1.5 μg m^{-3}). Zhang et al. (2008) also measured EC at Zhuzhang with an annual average concentration very similar to that reported to by Qu et al. (2008) (0.34 μg m^{-3}). The BC concentrations at Tengchong were also at the higher end of the levels measured at a background site in Kosan, Korea (80–430 ng m^{-3}) (Kim et al., 2000). These observations indicate the significant impact of long-range transported pollutants on this part of the Tibetan Plateau.

3.4. Carbonaceous and ionic species

Table 2 summarizes the average concentrations of OC, EC and water-soluble inorganic ions. The temporal patterns of OC, EC and SO_4^{2-} concentrations (Fig. 7) were similar to those observed for aerosol mass and BC, with low values corresponding to days with precipitation and significant build-up of concentrations in between those periods, although one needs to keep in mind that the number of filter-based samples was lower than the number of data points obtained with the continuous analysers. The chemical composition of the ambient aerosol was dominated by OC, EC and SO_4^{2-}. Average OC concentrations were 4.3 μg m^{-3} in $PM_{2.5}$ and 5.8 μg m^{-3} in PM_{10}, while those for EC were 1.1 μg m^{-3} and 1.5 μg m^{-3}, respectively. The corresponding values of SO_4^{2-} were 2.1 and 2.4 μg m^{-3}, respectively. The concentrations of other ionic species, such as NO_3^-, Ca^{2+}, Na^+, NH_4^+ and K^+, were lower, with typical values of less than 1 μg m^{-3} (Table 2).

Figure 8 shows the concentrations of OC, EC and all inorganic ions measured on 17 and 23 April and 4 and 13 May for evaluation of the change in concentrations before, during and after the episodic events mentioned in the previous section. It is noteworthy that OC, EC, SO_4^{2-} and NO_3^- were the species with the highest concentrations on 23 April and 4 May, while during the cleaner periods (17 April and 13 May) the predominant species were OC, EC, SO_4^{2-} and Na^+. For instance, fine-particle ($PM_{2.5}$) OC reached 11.4 and 9.9 μg m^{-3} and EC peak concentrations were 2.7 and 2.2 μg m^{-3} on 23 April and 4 May, respectively. Sulfate concentrations reached peak values of 3.5 and 2.6 μg m^{-3} on those days, respectively. The PM_{10} concentrations showed the same patterns as the respective $PM_{2.5}$ levels.

In order to illustrate the enrichment of ionic and carbonaceous species during the high-concentration episodes Fig. 9 shows normalized concentrations expressed as the ratio of the values on 23 April and 4 May over the average concentrations of the whole study period. It is notable that OC, EC, K^+, NO_3^- and NH_4^+ (especially on 4 May) were the species with the highest enhancements (around 200%) during these episodic events. Sulfate also showed consistent enhancement during both events, yet to a lesser extent. The NH_4^+ concentrations on 4 May showed an enrichment ratio of more than five in both $PM_{2.5}$ and PM_{10}. In a recent study, NH_4^+ was observed with high abundance in smoke aerosol derived from rice straw burning (Engling et al., 2009), while NH_4^+, K^+, NO_3^- and SO_4^{2-} were reported as the major water-soluble inorganic ions in aerosol influenced by post-harvest biomass burning in Korea (Ryu et al., 2004). These findings are consistent with the results of the trajectory analyses and the observations from the fire maps, indicating that burning activities, for example, in form of agricultural residue burning, in the upwind direction of Tengchong had important contributions to the ambient aerosol burden and BC in particular. Possible local influence from residential biofuel use (e.g. for cooking or heating) in Tengchong city was likely minimal due to the shielding effect of another mountain located between the sampling site and the urban area, in addition to the fact that the city was situated downwind of the sampling site based on the predominantly westerly winds during the study period. On the other hand, slight influence of burning activities in the surrounding mountain villages cannot be excluded, as mentioned above (Section 3.1).

Table 2. Average concentrations (μg m^{-3}) of OC, EC and water-soluble inorganic ions and their standard deviations (stdev).

		Na^+	NH_4^+	K^+	Mg^{2+}	Ca^{2+}	F^-	NO_2^-	NO_3^-	SO_4^{2-}	OC	EC
$PM_{2.5}$	Average	1.0	0.2	0.2	0.0	0.6	0.0	0.2	0.5	2.1	4.3	1.1
	Stdev	(0.3)	(0.3)	(0.1)	(0.0)	(0.2)	(0.0)	(0.3)	(0.3)	(0.7)	(3.8)	(0.8)
PM_{10}	Average	1.1	0.2	0.3	0.1	1.0	0.0	0.3	1.1	2.4	5.8	1.5
	Stdev	(0.3)	(0.3)	(0.1)	(0.0)	(0.3)	(0.0)	(0.3)	(0.7)	(0.8)	(4.4)	(1.0)

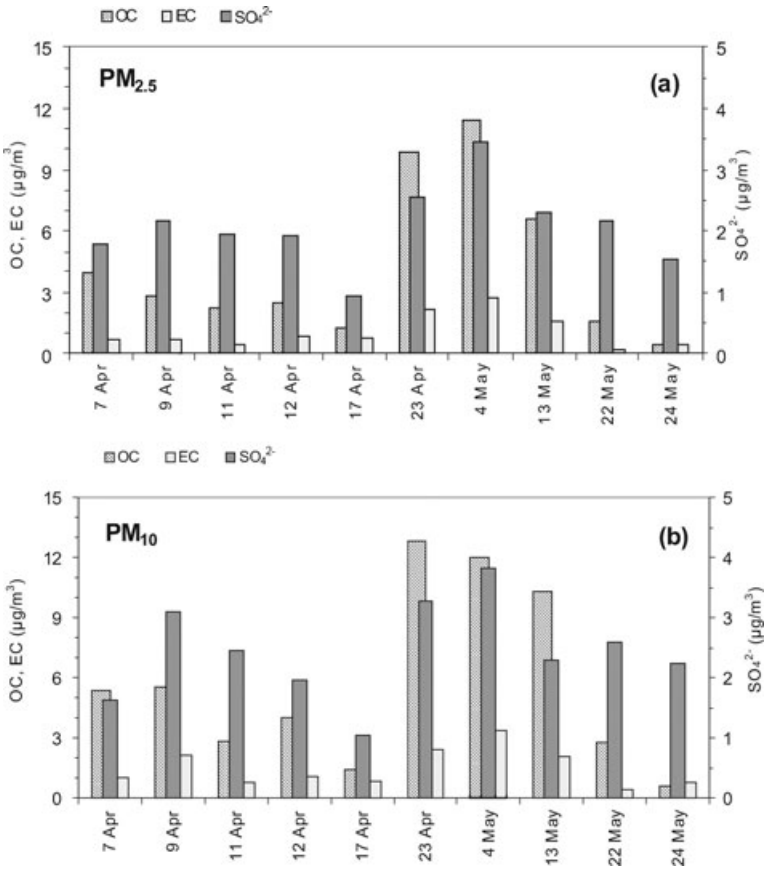

Fig. 7. Concentrations of OC, EC and SO_4^{2-} in $PM_{2.5}$ (a) and PM_{10} (b) for 10 selected days during the experiment period.

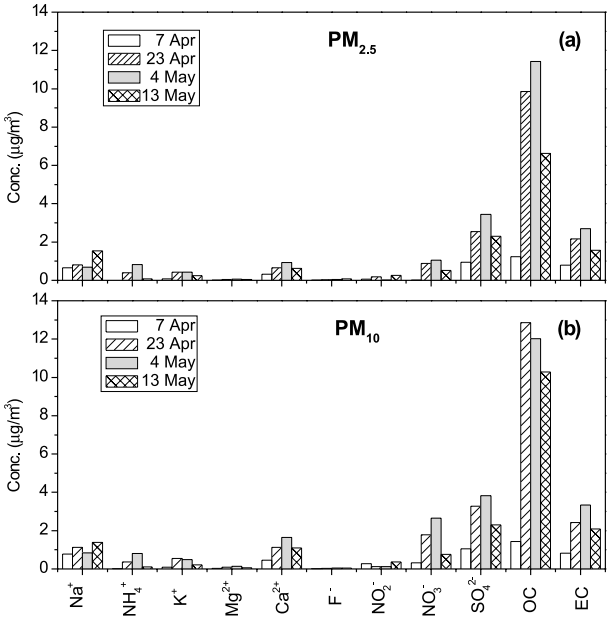

Fig. 8. Concentrations of OC, EC and ionic species in $PM_{2.5}$ (a) and PM_{10} (b) on 17 and 23 April and 4 and 13 May.

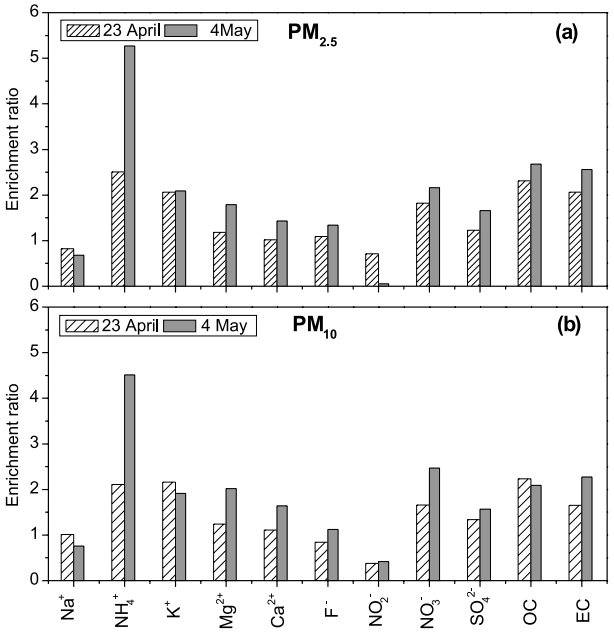

Fig. 9. Enrichment ratios of OC, EC and ionic species in $PM_{2.5}$ (a) and PM_{10} (b) during the episodic events on 23 April and 4 May, normalized to the average values from the entire experiment period.

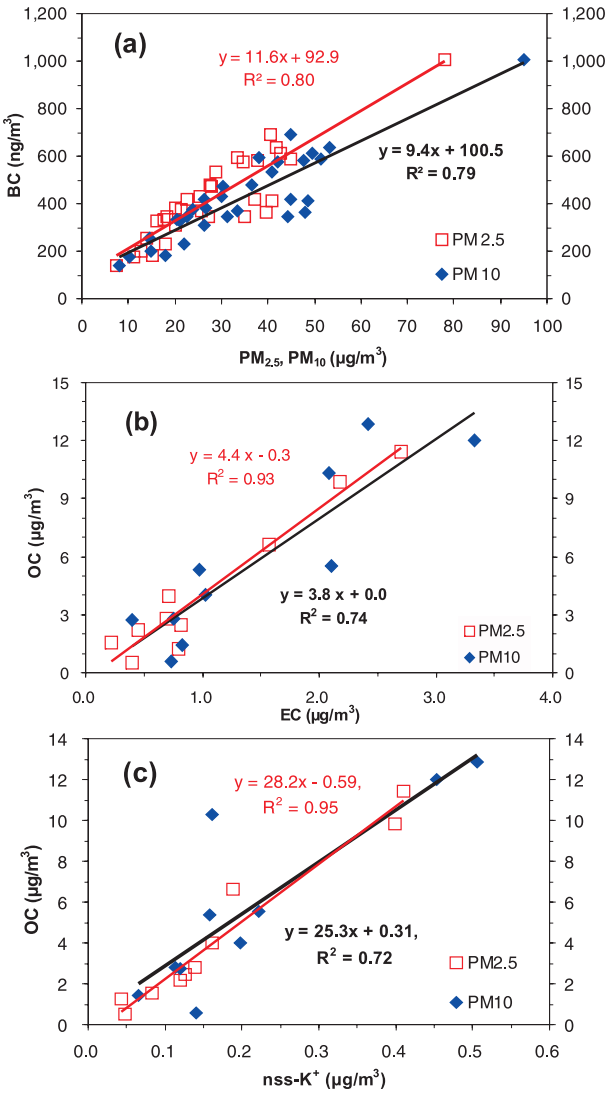

Fig. 10. Correlations between BC and $PM_{2.5}$ as well as PM_{10} mass concentrations (a), OC and EC (b) and OC and nss-K^+ in $PM_{2.5}$ and PM_{10} (c).

3.5. *Sources of carbonaceous aerosol*

Good correlations between $PM_{2.5}$ as well as PM_{10} mass and BC concentrations were found with the square of correlation coefficients (R^2) of 0.80 and 0.79 (Fig. 10a), respectively, based on daily average values measured with the on-line continuous analysers, indicating important contributions to the ambient aerosol from combustion processes. The origins of aerosols can also be evaluated by the relationship between OC and EC (Cao et al., 2003; Cheng et al., 2006). In this study, strong correlation was observed between OC and EC, with R^2 of 0.93 for $PM_{2.5}$ and 0.74 for PM_{10} and corresponding regression slopes of 4.4 and 3.8, respectively (Fig. 10b). The good correlation between OC and EC implies common sources for both carbonaceous species. EC (or BC) originates primarily from incomplete combustion of fossil fuels such as coal, diesel and gasoline, as well as biomass/biofuel burning. These processes are also major sources of OC. Thus, contributions from combustion processes to the ambient PM in this part of the Tibetan Plateau appear to have been important during the study period. Interestingly, an examination of the relationship between BC and NO_y revealed poor correlation (not shown), suggesting that high-temperature combustion processes, such as those in industrial operations and vehicle engines, were not significant sources of the carbonaceous aerosol at Tengchong. Therefore, low temperature combustion of biomass and/or biofuels was likely the dominant source of EC (or BC) at Tengchong during spring time, as will be further discussed below.

A considerable fraction of organic aerosols can also be formed through oxidation of volatile organic compounds derived from various anthropogenic as well as biogenic emission sources. Specifically, in remote and rural areas the fraction of secondary organic aerosol in the carbonaceous aerosol mass can be substantial with contributions of up to 80% (Zhang et al., 2007; Hallquist et al., 2009). In addition, primary biogenic aerosol (PBA) species may constitute a sizeable portion of OC, particularly in coarse PM. The relatively weak correlation between OC and EC in PM_{10} at Tengchong also indicates additional source types, such as PBA. Moreover, relatively high OC/EC ratios (3.13 and 2.63 for $PM_{2.5}$ and PM_{10}, respectively) confirm that biogenic (both primary and secondary) and/or biomass-burning processes had important contributions to the measured aerosol at Tengchong.

3.6. *Biomass/biofuel combustion sources*

Non-sea-salt-potassium (nss-K^+, $C_{nss-K+} = C_{K+} - 0.0355 \times C_{Na+}$) (Lai et al., 2007) is commonly used as source tracer for biomass-burning activities. The OC/nss-K^+ ratio can therefore be used in a first approximation to distinguish biomass burning from other OC sources. In this study, the OC/nss-K^+ ratios ranged from 10.2 to 35.3 in $PM_{2.5}$ and from 4.1 to 63.7 in PM_{10}. The correlations between OC and nss-K^+ were excellent in both $PM_{2.5}$ and PM_{10}, while R^2 in $PM_{2.5}$ (0.95) was noticeably higher than that in PM_{10} (0.72) (Fig. 10c). The linear regression slopes were 28.2 and 25.3 for $PM_{2.5}$ and PM_{10}, respectively. These values are higher (factor of ~ 5) than, for example, those observed during the burning season in Beijing (Duan et al., 2004). Since the majority of biomass-burning smoke particles is typically present in the fine mode, as shown in previous source emission and ambient studies (Engling et al., 2006; Herckes et al., 2006), the correlation between OC and nss-K^+ in $PM_{2.5}$ is expected to be better than that in PM_{10}, which was the case in this study. Moreover, additional sources contribute to the coarse portion of nss-K^+ in PM_{10}. Thus, these results provide further indication of biomass-burning emissions as a major source of the aerosol in this remote part of the Tibetan Plateau, which is also supported

by the observations of fire activity in the source regions (Fig. 5) and air mass history (Fig. 6).

Novakov et al. (2000) investigated the origins of filter-based carbonaceous aerosols sampled on board aircraft over the Indian Ocean by comparing BC/TC (TC = total carbon; hereafter we will use the term EC instead of BC in order to avoid possible confusion with the BC concentrations measured by the continuous analyser in this study), EC/OC, K^+/EC, SO_4^{2-}/TC and SO_4^{2-}/EC ratios to those measurements reported for urban, industrial and rural sites, as well as regions with biomass-burning influence, on the Indian Peninsula (Pakistan) and regions downwind of industrialized areas of Japan and western Europe. It is interesting that the EC/TC and OC/EC ratios at Tengchong were very close to the corresponding ratios at various sites in Lahore, Pakistan, while SO_4^{2-}/EC in PM_{10} and K^+/EC ratios were similar to those observed over the Indian Ocean (Smith and Harrison, 1996). The apparent influence of those regions on the air masses reaching Tengchong during this study is confirmed by the backward trajectories (Fig. 6). On the other hand, the EC/TC ratios (0.23 ± 0.10 and 0.24 ± 0.13 for $PM_{2.5}$ and PM_{10}, respectively) were approximately two times those reported for biomass-burning regions in northern India (0.13) (Ram and Sarin, 2010).

Higher OC/EC ratios indicate influence from biomass-burning sources (as well as biogenic sources), while lower ratios are attributed to fossil-fuel combustion (Ram and Sarin, 2010). For example, an average OC/EC ratio of 6.6 was reported for biomass combustion (Saarikoski et al., 2008) and 7.3 for wood burning emissions in particular (Sandradewi et al., 2008), whereas a low OC/EC ratio of 1.1 was found for traffic emissions (Sandradewi et al., 2008). Based on the low ratios of OC/EC, Novakov et al. (2000) suggested that fossil fuel combustion was the major source of carbonaceous aerosols, including BC, over the Indian Ocean. However, more recent studies have revealed biomass/biofuel combustion as the key source of carbonaceous aerosol in this region (Rengarajan et al., 2007; Aunan et al., 2009; Gustafsson et al., 2009; Stone et al., 2010).

A noticeably high SO_4^{2-}/EC ratio in $PM_{2.5}$ (2.47) and to a lesser extent in PM_{10} (1.57), yet suggests that aerosol contributions from fossil fuel combustion cannot be ignored in this part of the Tibetan Plateau. However, due to the large variability in such elemental ratios depending on specific combustion conditions, it is difficult to draw reliable conclusions from these ratios. In fact, more advanced methods need to be used to identify the contributions from fossil fuel combustion in Tengchong, such as radiocarbon (^{14}C) measurements which allow to differentiate between carbonaceous aerosol species derived from biomass burning (contemporary ^{14}C signal) and fossil fuel combustion (extinct ^{14}C) (Szidat et al., 2007; Gustafsson et al., 2009).

4. Conclusions

There is very limited observational data reported on aerosols and associated chemical components (BC in particular) for the Tibetan Plateau. The data observed in this study provide important preliminary insights into the chemical composition and the sources of aerosols in this remote part of the Tibetan Plateau, which plays a fundamental role in altering the large-scale atmospheric circulation of Asia and the global climate. Our results unveiled a substantial regional build-up of BC and other aerosol components during the dry period, accompanied by fire activities and transport of pollution from the nearby regions of SE Asia and the northern part of the Indian Peninsula. The concentrations of BC and aerosol mass during episodic events were comparable to those reported for certain large Asian cities.

The findings from this study highlight the complex source characteristics of aerosols and BC in particular. The chemical composition of the ambient aerosol was characterized by high OC, EC and SO_4^{2-} content with characteristic OC/nss-K^+ ratios, indicating significant contributions of biomass-burning emissions. The possible impact of anthropogenic emissions and biomass burning in particular, on this vulnerable region of the Tibetan Plateau certainly deserves more scientific attention. Future investigations need to assess the temporal and spatial variations of aerosol chemical and physical properties, including more comprehensive chemical speciation and measurements of optical aerosol properties throughout all seasons and simultaneously at multiple locations across the vast Tibetan Plateau. Specifically, further studies are necessary to identify the influence of fossil fuel combustion sources and to quantify both fossil fuel and biomass/biofuel combustion contributions to the aerosol burden by using novel methods such as radiocarbon measurements.

5. Acknowledgments

This field study was supported by a research grant of the Hong Kong Polytechnic University (AS504). Parts of this study were supported by the Natural Science Foundation of China (No. 40875075). We would like to thank Dr. C.S. Zhao of Peking University for lending us the BC analyser and for his support during the field campaign.

References

Ahmed, T., Dutkiewicz, V. A., Shareef, A., Tuncel, G., Tuncel, S. and co-authors. 2009. Measurement of black carbon (BC) by an optical method and a thermal-optical method: intercomparison for four sites. *Atmos. Environ.* **43**, 6305–6311.

Andreae, M. O. and Gelencsér, A. 2006. Black carbon or brown carbon? The nature of light-absorbing carbonaceous aerosols. *Atmos. Chem. Phys.* **6**, 3131–3148.

Aunan, K., Berntsen, T. K., Myhre, G., Rypdal, K., Streets, D. G. and co-authors. 2009. Radiative forcing from household fuel burning in Asia. *Atmos. Environ.* **43**, 5674–5681.

Babu, S. S. and Moorthy, K. K. 2002. Aerosol black carbon over a tropical coastal station in India. *Geophys. Res. Lett.* **29**, doi:10.1029/2002gl015662.

Cao, J. J., Lee, S. C., Ho, K. F., Zhang, X. Y., Zou, S. C. and co-authors. 2003. Characteristics of carbonaceous aerosol in Pearl River Delta Region, China during 2001 winter period. *Atmos. Environ.* **37**, 1451–1460.

Cao, J. J., Lee, S. C., Chow, J. C., Watson, J. G., Ho, K. F. and co-authors. 2007. Spatial and seasonal distributions of carbonaceous aerosols over China. *J. Geophys. Res.* **112**, doi:10.1029/2006jd008205.

Cao, J.-J., Zhu, C.-S., Chow, J. C., Watson, J. G., Han, Y.-M. and co-authors. 2009. Black carbon relationships with emissions and meteorology in Xi'an, China. *Atmos. Res.* **94**, 194–202.

Chan, C. Y., Chan, L. Y., Harris, J. M., Oltmans, S. J., Blake, D. R. and co-authors. 2003. Characteristics of biomass burning emission sources, transport, and chemical speciation in enhanced springtime tropospheric ozone profile over Hong Kong. *J. Geophys. Res.* **108**, doi:10.1029/2001jd001555.

Chan, C. Y., Wong, K. H., Li, Y. S., Chan, L. Y. and Zheng, X. D. 2006. The effects of Southeast Asia fire activities on tropospheric ozone, trace gases and aerosols at a remote site over the Tibetan Plateau of Southwest China. *Tellus B* **58**, 310–318.

Chen, L. W.A., Doddridge, B. G., Dickerson, R. R., Chow, J. C., Mueller, P. K. and co-authors. 2001. Seasonal variations in elemental carbon aerosol, carbon monoxide and sulfur dioxide: implications for sources. *Geophys. Res. Lett.* **28**, 1711–1714.

Cheng, Y., Lee, S. C., Ho, K. F., Wang, Y. Q., Cao, J. J. and co-authors. 2006. Black carbon measurement in a coastal area of south China. *J. Geophys. Res.* **111**, doi:10.1029/2005jd006663.

Chow, J. C. and Watson, J. G. 2002. Review of PM2.5 and PM10 Apportionment for fossil fuel combustion and other sources by the Chemical Mass Balance Receptor Model. *Energ. Fuel.* **16**, 222–260.

Chow, J. C., Watson, J. G., Pritchett, L. C., Pierson, W. R., Frazier, C. A. and co-authors. 1993. The DRI thermal/optical reflectance carbon analysis system: description, evaluation and applications in U.S. air quality studies. *Atmos. Environ.* **27A**, 1185–1201.

Duan, F., Liu, X., Yu, T. and Cachier, H. 2004. Identification and estimate of biomass burning contribution to the urban aerosol organic carbon concentrations in Beijing. *Atmos. Environ.* **38**, 1275–1282.

Duncan, B. N., Martin, R. V., Staudt, A. C., Yevich, R. and Logan, J. A. 2003. Interannual and seasonal variability of biomass burning emissions constrained by satellite observations. *J. Geophys. Res.* **108**, doi:10.1029/2002jd002378.

Engling, G. and Gelencsér, A. 2010. Atmospheric Brown Clouds: from local air pollution to climate change. *Elements* **6**, 223–228, doi:10.2113/gselements.6.4.223.

Engling, G., Carrico, C. M., Kreidenweis, S. M., Collett Jr, J. L., Day, D. E. and co-authors. 2006. Determination of levoglucosan in biomass combustion aerosol by high-performance anion-exchange chromatography with pulsed amperometric detection. *Atmos. Environ.* **40**, S299–S311.

Engling, G., Lee, J. J., Tsai, Y.-W., Lung, S.-C.C., Chou, C. C.K. and co-authors. 2009. Size-Resolved anhydrosugar composition in smoke aerosol from controlled field burning of rice straw. *Aerosol Sci. Technol.* **43**, 662–672.

Gadde, B., Bonnet, S., Menke, C. and Garivait, S. 2009. Air pollutant emissions from rice straw open field burning in India, Thailand and the Philippines. *Environ. Pollut.* **157**, 1554–1558.

Gelencsér, A. 2004. Carbonaceous aerosol. In: *Atmosperic and Oceanographic Sciences Library* Volume 30. Springer, Dordrecht, ISBN: 1–4020-2886–5.

Gustafsson, O., Krusa, M., Zencak, Z., Sheesley, R. J., Granat, L. and co-authors. 2009. Brown clouds over South Asia: biomass or fossil fuel combustion? *Science* **323**, 495–498.

Hallquist, M., Wenger, J. C., Baltensperger, U., Rudich, Y., Simpson, D. and co-authors. 2009. The formation, properties and impact of secondary organic aerosol: current and emerging issues. *Atmos. Chem. Phys.* **9**, 5155–5236.

Hansen, A. D.A., Rosen, H. and Novakov, T. 1984. The aethalometer—An instrument for the real-time measurement of optical absorption by aerosol particles. *Sci. Total Environ.* **36**, 191–196.

Hansen, A. D.A., Lowenthal, D. H., Chow, J. C. and Watson, J. G. 2001. Black carbon aerosol at McMurdo station, Antarctica. *J. Air Waste Manage. Assoc.* **51**, 593–600.

Herckes, P., Engling, G., Kreidenweis, S. M. and Collett, J. L. 2006. Particle size distributions of organic aerosol constituents during the 2002 Yosemite Aerosol Characterization Study. *Environ. Sci. Technol.* **40**, 4554–4562.

Jacob, D. J., Crawford, J. H., Kleb, M. M., Connors, V. S., Bendura, R. J. and co-authors. 2003. Transport and Chemical Evolution over the Pacific (TRACE-P) aircraft mission: design, execution, and first results. *J. Geophys. Res.* **108**, doi:10.1029/2002jd003276.

Kim, Y. P., Moon, K. C. and Lee, J. H. 2000. Organic and elemental carbon in fine particles at Kosan, Korea. *Atmos. Environ.* **34**, 3309–3317.

Lai, S. C., Zou, S. C., Cao, J. J., Lee, S. C. and Ho, K. F. 2007. Characterizing ionic species in PM2.5 and PM10 in four Pearl River Delta cities, South China. *J. Environ. Sci.* **19**, 939–947.

Lelieveld, J., Crutzen, P. J., Ramanathan, V., Andreae, M. O., Brenninkmeijer, C. A.M. and co-authors. 2001. The Indian Ocean Experiment: widespread air pollution from South and Southeast Asia. *Science* **291**, 1031–1036.

Li, Q. B., Jiang, J. H., Wu, D. L., Read, W. G., Livesey, N. J. and co-authors. 2005. Convective outflow of South Asian pollution: a global CTM simulation compared with EOS MLS observations. *Geophys. Res. Lett.* **32**, doi:10.1029/2005gl022762.

Ma, Y., Wang, Y., Wu, R., Hu, Z., Yang, K. and co-authors. 2009. Recent advances on the study of atmosphere-land interaction observations on the Tibetan Plateau. *Hydr. Earth Syst. Sci.* **13**, 1103–1111.

Maenhaut, W., De Ridder, D. J.A., Fernandez-Jimenez, M. T., Hooper, M. A., Hooper, B. and co-authors. 2002. Long-term observations of regional aerosol composition at two sites in Indonesia. *Nucl. Instrum. Meth. B.* **189**, 259–265.

Marinoni, A., Cristofanelli, P., Calzolari, F., Roccato, F., Bonafe, U. and co-authors. 2008. Continuous measurements of aerosol physical parameters at the Mt. Cimone GAW Station (2165 m asl, Italy). *Sci. Total Environ.* **391**, 241–251.

Menon, S., Hansen, J., Nazarenko, L. and Luo, Y. F. 2002. Climate effects of black carbon aerosols in China and India. *Science* **297**, 2250–2253.

Novakov, T., Andreae, M. O., Gabriel, R., Kirchstetter, T. W., Mayol-Bracero, O. L. and co-authors. 2000. Origin of carbonaceous aerosols over the tropical Indian Ocean: biomass burning or fossil fuels? *Geophys. Res. Lett.* **27**, 4061–4064.

Pant, P., Hegde, P., Dumka, U. C., Saha, A., Srivastava, M. K. and co-authors. 2006. Aerosol characteristics at a high-altitude location during ISRO-GBP Land Campaign-II. *Curr. Sci.* **91**, 1053–1061.

Qu, W. J., Zhang, X. Y., Arimoto, R., Wang, D., Wang, Y. Q. and co-authors. 2008. Chemical composition of the background aerosol at two sites in southwestern and northwestern China: potential influences of regional transport. *Tellus B* **60**, 657–673.

Qu, W. J., Zhang, X. Y., Arimoto, R., Wang, Y. Q., Wang, D. and co-authors. 2009. Aerosol background at two remote CAWNET sites in western China. *Sci. Total Environ.* **407**, 3518–3529.

Ram, K. and Sarin, M. M. 2010. Spatio-temporal variability in atmospheric abundances of EC, OC and WSOC over Northern India. *J. Aerosol Sci.* **41**, 88–98.

Ram, K., Sarin, M. M. and Hegde, P. 2008. Atmospheric abundances of primary and secondary carbonaceous species at two high-altitude sites in India: sources and temporal variability. *Atmos. Environ.* **42**, 6785–6796.

Ramanathan, V. and Carmichael, G. 2008. Global and regional climate changes due to black carbon. *Nat. Geosci.* **1**, 221–227.

Ramanathan, V., Ramana, M. V., Roberts, G., Kim, D., Corrigan, C. and co-authors. 2007. Warming trends in Asia amplified by brown cloud solar absorption. *Nature* **448**, 575–578.

Rengarajan, R., Sarin, M. M. and Sudheer, A. K. 2007. Carbonaceous and inorganic species in atmospheric aerosols during wintertime over urban and high-altitude sites in North India. *J. Geophys. Res.* **112**, doi:10.1029/2006jd008150.

Ryu, S. Y., Kim, J. E., Zhuanshi, H., Kim, Y. J. and Kang, G. U. 2004. Chemical composition of post-harvest biomass burning aerosols in Gwangju, Korea. *J. Air Waste Manage. Assoc.* **54**, 1124–1137.

Saarikoski, S., Timonen, H., Saarnio, K., Aurela, M., Jarvi, L. and co-authors. 2008. Sources of organic carbon in fine particulate matter in northern European urban air. *Atmos. Chem. Phys.* **8**, 6281–6295.

Sandradewi, J., Prevot, A. S.H., Weingartner, E., Schmidhauser, R., Gysel, M. and co-authors. 2008. A study of wood burning and traffic aerosols in an Alpine valley using a multi-wavelength Aethalometer. *Atmos. Environ.* **42**, 101–112.

Sheesley, R. J., Schauer, J. J., Chowdhury, Z., Cass, G. R. and Simoneit, B. R.T. 2003. Characterization of organic aerosols emitted from the combustion of biomass indigenous to South Asia. *J. Geophys. Res.* **108**, doi:10.1029/2002jd002981.

Slowik, J. G., Cross, E. S., Han, J.-H., Davidovits, P., Onasch, T. B. and co-authors. 2007. An inter-comparison of instruments measuring black carbon content of soot particles. *Aerosol Sci. Technol.* **41**, 295–314.

Smith, D. J.T. and Harrison, R. M. 1996. Concentrations, trends and vehicle source profile of polynuclear aromatic hydrocarbons in the U.K. atmosphere. *Atmos. Environ.* **30**, 2513–2525.

Stone, E. A., Lough, G. C., Schauer, J. J., Praveen, P. S., Corrigan, C. E. and co-authors. 2007. Understanding the origin of black carbon in the atmospheric brown cloud over the Indian Ocean. *J. Geophys. Res.* **112**, doi: 10.1029/2006jd008118.

Stone, E. A., Schauer, J. J., Pradhan, B. B., Dangol, P. M., Habib, G. and co-authors. 2010. Characterization of emissions from South Asian biofuels and application to source apportionment of carbonaceous aerosol in the Himalayas. *J. Geophys. Res.* **115**, doi:10.1029/2009jd011881.

Streets, D. G., Yarber, K. F., Woo, J. H. and Carmichael, G. R. 2003. Biomass burning in Asia: annual and seasonal estimates and atmospheric emissions. *Global Biogeochem. Cycles* **17**, doi:10.1029/2003gb002040.

Szidat, S., Prevot, A. S.H., Sandradewi, J., Alfarra, M. R., Synal, H. A. and co-authors. 2007. Dominant impact of residential wood burning on particulate matter in Alpine valleys during winter. *Geophys. Res. Lett.* **34**, doi:10.1029/2006GL028325.

Tang, J., Wen, Y., Zhou, L., Qi, D., Zheng, M., Leil, T. and Wallgren, E. 1999. Observational study of black carbon in clean air area of western China. *Quart. J. Appl. Met.*, **10**, 160–170 (in Chinese).

Tripathi, S. N., Dey, S., Tare, V. and Satheesh, S. K. 2005. Aerosol black carbon radiative forcing at an industrial city in northern India. *Geophys. Res. Lett.* **32**, doi:10.1029/2005gl022515.

Wang, X. D., Zhong, X. H., Liu, S. Z., Liu, J. G., Wang, Z. Y. and co-authors. 2008. Regional assessment of environmental vulnerability in the Tibetan Plateau: development and application of a new method. *J. Arid. Environ.* **72**, 1929–1939.

Ye, D. Z. and Wu, G. X. 1998. The role of the heat source of the Tibetan Plateau in the general circulation. *Meteorol. Atmos. Phys.* **67**, 181–198.

Zhang, Q., Jimenez, J. L., Canagaratna, M. R., Allan, J. D., Coe, H. and co-authors. 2007. Ubiquity and dominance of oxygenated species in organic aerosols in anthropogenically-influenced Northern Hemisphere midlatitudes. *Geophys. Res. Lett.* **34**, doi:10.1029/2007GL029979.

Zhang, X. Y., Wang, Y. Q., Zhang, X. C., Guo, W. and Gong, S. L. 2008. Carbonaceous aerosol composition over various regions of China during 2006. *J. Geophys. Res.* **113**, doi:10.1029/2007jd009525.